

# Effect of Foundry Variables on the Casting Quality of As-Cast LM25 Aluminium Alloy

Mohammad Sharear Kabir, Ehsan Ahmed Ashrafi, Tamzid Ibn Minhaj, Md Moinul Islam

**Abstract**— The effect of foundry variables, such as mold materials and pouring temperature on the microstructure, dendrite arm spacing, percentage porosity and mechanical properties of as-cast LM25 Al alloy was investigated. The microstructure of the as-cast samples was characterized by optical microscopy. The results showed that the secondary dendrite arm spacing (SDAS,  $\lambda$ ) is well refined by pouring at higher temperatures in metal mold compared to greensand mold. The SDAS decreases with increasing pouring temperature due to multiplication of nucleation sites in the superheating liquid melt. The percentage porosity of the cast specimens decreases with increasing pouring temperatures and is lowest for metal mold at highest pouring temperature. The mechanical properties of the as-cast LM25 Al alloy, such as hardness and ultimate tensile strength increases as pouring temperature increases. However, percentage elongation of the as-cast alloy decreases with increasing pouring temperatures. Among the mold materials, permanent metal mold casting has shown to impart better quality than greensand mold casting.

**Index Terms**— LM25 Al alloy, Pouring temperature, secondary dendrite arm spacing (SDAS,  $\lambda$ ), percentage porosity, permanent metal mold, greensand mold, mechanical property.

## I. INTRODUCTION

Aluminium and Aluminium alloy castings have dominated the automotive sector for decades [1]. Approximately two thirds of all aluminium castings are used in automotive industries and it continues to grow at the expense of iron castings. Although aluminium castings are significantly more expensive than ferrous castings, there is a continuing market requirement to reduce vehicle weight and to increase fuel efficiency. It is this requirement which drives the replacement of ferrous parts by aluminium. LM25 is a common purpose alloy of aluminium which finds application in the food, chemical, marine, electrical and many other industries and above all in the automotive industry for the manufacture of cylinder blocks and heads, and other engine and body castings [3]. Its potential uses are increased due to its availability in four conditions of heat treatment in both sand and chill castings. It is quite suitable for fairly thin castings as well and the production of castings in this alloy does not introduce any problems due to hot tearing.

Manuscript published on 30 August 2014.

\* Correspondence Author (s)

**Mohammad Sharear Kabir**, Department of Materials and Metallurgical Engineering, Bangladesh University of Engineering and Technology, Dhaka - 1000, Bangladesh.

**Ehsan Ahmed Ashrafi**, Department of Materials and Metallurgical Engineering, Bangladesh University of Engineering and Technology, Dhaka - 1000, Bangladesh.

**Tamzid Ibn Minhaj**, Department of Materials and Metallurgical Engineering, Bangladesh University of Engineering and Technology, Dhaka - 1000, Bangladesh.

**Md Moinul Islam**, Department of Materials and Metallurgical Engineering, Bangladesh University of Engineering and Technology, Dhaka - 1000, Bangladesh.

© The Authors. Published by Blue Eyes Intelligence Engineering and Sciences Publication (BEIESP). This is an open access article under the CC-BY-NC-ND license <http://creativecommons.org/licenses/by-nc-nd/4.0/>

It has a good resistance to corrosion and has a high strength and also offers good machinability [4]. It is imperative to possess knowledge about solidification phenomena and their effect on mechanical properties while designing cast automotive parts. Knowledge of solidification phenomena can help a designer to ensure sound casting and this in turn will ensure that the casting will achieve the desired properties for its intended application [5]–[8]. The solidification of cast aluminum alloys start with separation of primary  $\alpha$ - phase from the liquid. When the temperature lowers after nucleation, the primary phase grows as solid crystals having dendritic shape. When the eutectic temperature has been reached, the solidification proceeds at constant temperature with the formation of the eutectic solid phase in the space left between dendritic arms. The secondary dendrite arm spacing (SDAS), defined as the distance between the protruding adjacent secondary arms of a dendrite, has been used in recent years to characterize the metallurgical structure of cast materials. It is well known that various cooling rates during solidification can lead to variation in the amount and various morphological characteristics of as-cast structures, which in turn can lead to different mechanical properties [6], [9]–[11]. Castings having a finer microstructure show better tensile and fatigue properties, particularly for cast aluminum alloys, this improvement is related to a lower SDAS value. Studies on the effect of SDAS on tensile properties report that the tensile strength and ductility are found to decrease with increasing value of SDAS [12]. Because of the evident importance of SDAS, many automotive companies have included SDAS values in engineering data for aluminum castings. Increasing the strict control over SDAS enables the production of castings with improved properties [13]. In the present work, the influence of foundry variables such as mold materials and pouring temperatures on the microstructure and mechanical properties of as-cast LM25 Al alloy have been determined and studied. A relationship was drawn between casting variables such as pouring temperatures, SDAS and mechanical properties such as UTS, %EL and Hardness). Modelling of the alloys were done using JMatPro version 4.1. Thermodynamic calculations of changes in phases with temperature in both equilibrium and non-equilibrium solidification conditions were performed. From these calculations the identity and amount of different phases in the alloy at different temperatures were predicted.

## II. MATERIALS AND TEST PROCEDURES

### A. Specimen Preparation

Four molds, two greensand molds and two metal molds were prepared in advance before melting the master alloy. About four kilograms of LM25 (BS 1490:1988 LM25) Al master alloy was melted in a graphite crucible placed in a gas fired pit furnace.



All the molds were preheated to required temperature. After using necessary fluxing and degassing agent (ammonium chloride), the liquid Al metal was poured in one greensand mold and in one metal mold at a pouring temperature of 900°C. When the temperature of the melt dropped down to 700°C, the remaining liquid metal was poured into a greensand mold and in a metal mold. The temperature readings were obtained by submerging a pyrometer rod into the molten liquid. The melt was continuously stirred to avoid non-uniform temperature distribution throughout the melt. After cooling the castings were removed from their respective gating systems. Thus two types of cast specimens were obtained corresponding to two different pouring temperatures, i.e. 900°C and 700°C.

**B. Microstructural analysis**

The specimens for microstructural analysis were machined to cylindrical shapes. Standard techniques were followed for the preparation for observation. Grinding was done on silicon carbide abrasive papers of various grit sizes, final polishing being done on a velvet cloth using a suspension of alumina (Al<sub>2</sub>O<sub>3</sub>) powder. The specimens were then washed and dried with acetone before observation. The microstructures were studied using a metallurgical microscope. Secondary dendrites were observed and length of secondary dendrite arm spacing (SDAS, λ) was calculated for all specimens as follows:

- a) A dendrite stem was selected where 5 or more secondary dendrite arms could be identified
- b) The length of the stem was measured and the number of secondary dendrite arms was counted
- c) SDAS was calculated [14] according to the formula:

$$\lambda = \frac{(L)}{(n)} \times \frac{1}{(V)} \tag{1}$$

- L – Length of dendrite stem
- n – No. of secondary dendrite arms
- V - Magnification

**C. Phase analysis**

Using JMatPro the evolution and of phases during solidification of LM25 alloy was identified. The presence of intermetallic phases and their solidification was also studied. Furthermore, the stoppage of solidification of few intermetallic phases was also identified.

**D. Calculation of porosity**

Cylindrical specimens were created from the broken/discarded tensile test bars after tensile testing and machined to bring about surface smoothness. Then mass and volume was calculated for each specimen to find out the apparent density. True density of the LM25 Al alloy as per BS 1490:1988 LM25 is 2.68 gm/cc. The % porosity was calculated as follows:

$$\% \text{ Porosity} = \frac{(\text{True density} - \text{Apparent density}) \times 100}{\text{True density}} \tag{2}$$

**E. Hardness test**

The hardness values of the samples were determined using the Brinell hardness tester. The Brinell hardness test was conducted by applying 500 kg load (L) for 30 seconds with a ball of 10 mm diameter (D) on the surface of the samples. Then the diameter of the impression (d) was measured by the

scale. Then the hardness was calculated by the equation given below:

$$\text{BHN} = \frac{L}{\pi D (D - \sqrt{D^2 - d^2})} \tag{3}$$

**F. Tensile test**

Four tensile specimens were machined from the four types of cast specimens according to ASTM B557 standards [15]. The tensile specimen is shown in Fig. 1 and the standard dimensions are shown in Table 1. From the tensile test UTS and %EL were recorded.

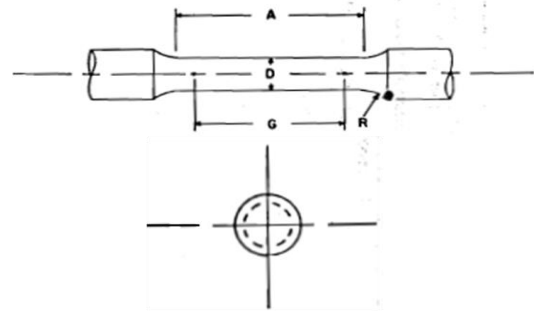


**Fig. 1 Standard 0.50 in Round Tension Test Specimen[15]**

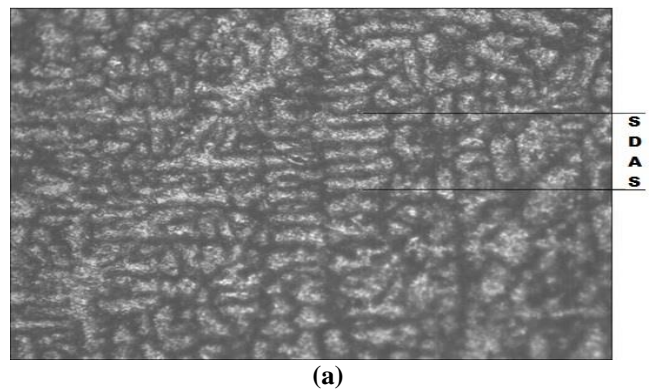
**Table 1 Standard ASTM B557 Tensile Test Specimen Dimensions in inches [15].**

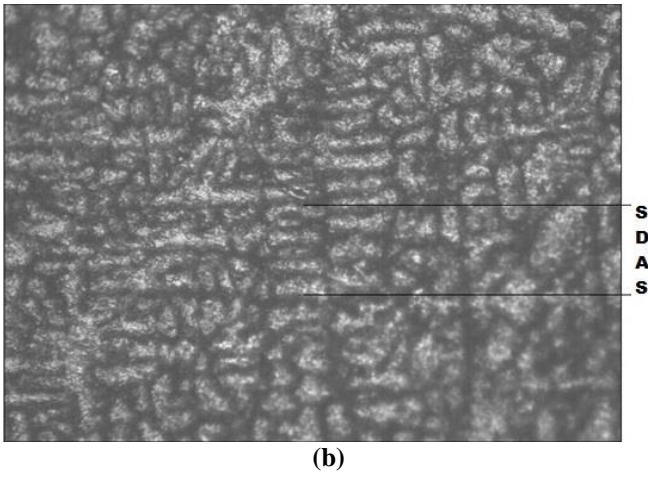
	Standard Specimen (inches)
Nominal Diameter	0.500
G – Gage length	2.000 ± 0.005
D – Diameter	0.500 ± 0.010
R – Radius of fillet	3/8
A – length of reduced section	2 1/4

**III. RESULTS AND DISCUSSIONS**

**A. Microstructural analysis**

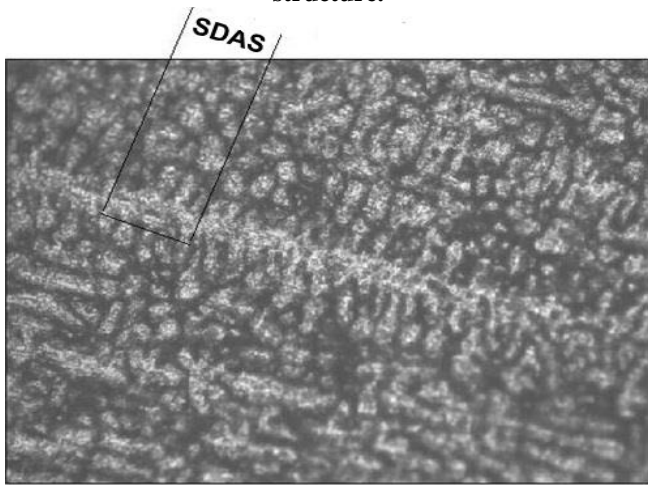
The optical microstructures of the LM25 alloy casted in greensand mold at pouring temperatures of 700°C and 900°C are shown in Fig. 2(a) and (b) and that of the alloy casted in metal mold at pouring temperatures of 700°C and 900°C are shown in Fig. 3(a) and (b).



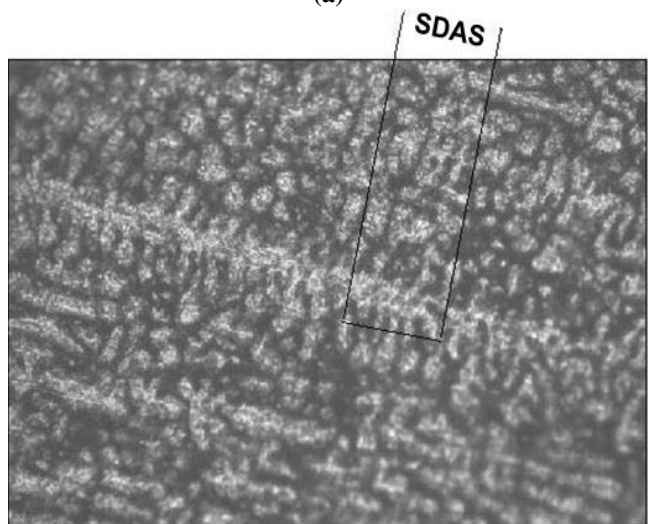


(b)

**Fig. 2 Microstructure [Magnification: 100X] of LM25 alloy casted in sand mold consisting of coarse dendrite structure.**



(a)



(b)

**Fig. 3 Microstructure [Magnification: 100X] of LM25 alloy casted in metal mold consisting of fine dendrite structure.**

The SDAS of all samples at different pouring temperatures for different casting molds are shown in Table 2, it can be seen that the SDAS decreases with increasing pouring temperature, meaning that the pouring temperature has a significant refining effect.

**Table 2 SDAS,  $\lambda$  values for different pouring temperature**

Type of mold	Pouring temperature	SDAS, $\lambda$ ( $\mu\text{m}$ )
Greensand	900°C	60
	700°C	69
Metal	900°C	55
	700°C	61

In conventional cast processing, the melt is usually poured at higher temperature, by about 50°C than its liquidus point [16]. The higher the temperature, the more is the activity of liquid metal, which results in more nucleating spots in the liquid metal. It is well known that the refinement is achieved by the multiplication of the nucleation sites in the liquid melt [16]. According to the solidification theory, the critical nucleus diameter is inversely proportion to the melt undercooling and the decreasing Gibbs free energy. Thus, the increasing undercooling will be beneficial for nucleation due to decreasing size of critical nucleation and also provide a larger crystallization driving force. This means that pouring at higher temperature will result in the formation of small nucleation sites in large numbers. On the contrary, pouring at low temperatures will result in the formation of nucleation sites in small numbers but they will be larger in size than the former. The SDAS is effectively reduced due to the increase in amount of the nucleation at high pouring temperature. Therefore, the SDAS is decreased with increasing pouring temperature. The SDAS is mainly dependent on the cooling rate and high cooling rate results in small SDAS. The cooling rate is also controlled by the type of mold used for casting. Metal molds allow higher cooling rates than greensand molds and consequently the SDAS of specimen cooled in metal mold is smaller than that in greensand mold.

**B. Phase analysis**

Using JMatPro thermodynamic calculations of changes in phases with temperature in equilibrium solidification conditions were made. The identity and amount of different phases in the alloy at different temperatures were predicted. From the Step Temperature calculation predicted in thermodynamic modeling using JMatPro, the evolution and abolition of different phases in the LM25 Al alloy are clearly observed in Fig. 4. It is evident that the Al phase starts to solidify first at 615°C. It can be seen at the right that most of the intermetallic phases are of Al, Si, Cu, Fe and Mg. In Fig. 5, we can see that the Silicon and Al-Fe-Si phase starts to solidify at 567°C. At 445°C, Al-Fe-Mg-Si phase ( $\text{Al}_8\text{FeMg}_3\text{Si}_6$ ) starts to grow and ends at 388°C with the evolution of  $\text{Mg}_2\text{Si}$  phase. The Mg-Si phase totally vanishes at 320°C, while another Al-Cu-Mg-Si ( $\text{Al}_5\text{Cu}_2\text{Mg}_3\text{Si}_6$ ) phase starts to grow at 370°C. So, those Magnesium and Silicon contents are transferred from the  $\text{Mg}_2\text{Si}$  phase to the new Al-Cu-Mg-Si phase. Another Al-Cu phase ( $\text{Al}_2\text{Cu}$ ) starts to evolve at 180°C. From this study, we can assume that the Al phase solidifies first and forms the dendrite, while the Silicon and other intermetallic phases remain in the inter-dendritic region.



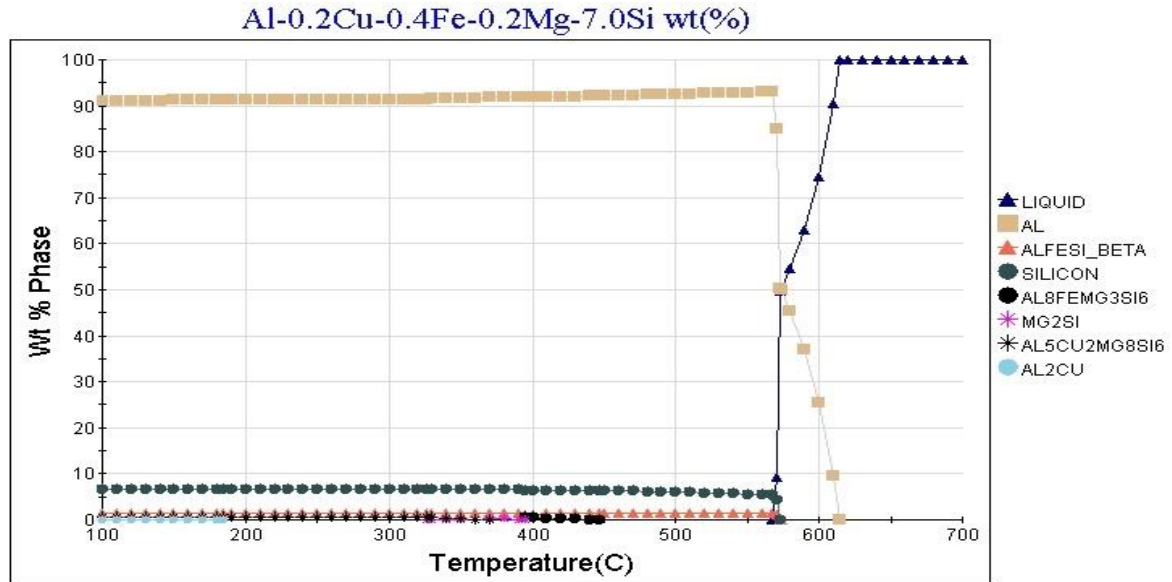


Fig. 4 Step Temperature Modeling of LM25 Alloy

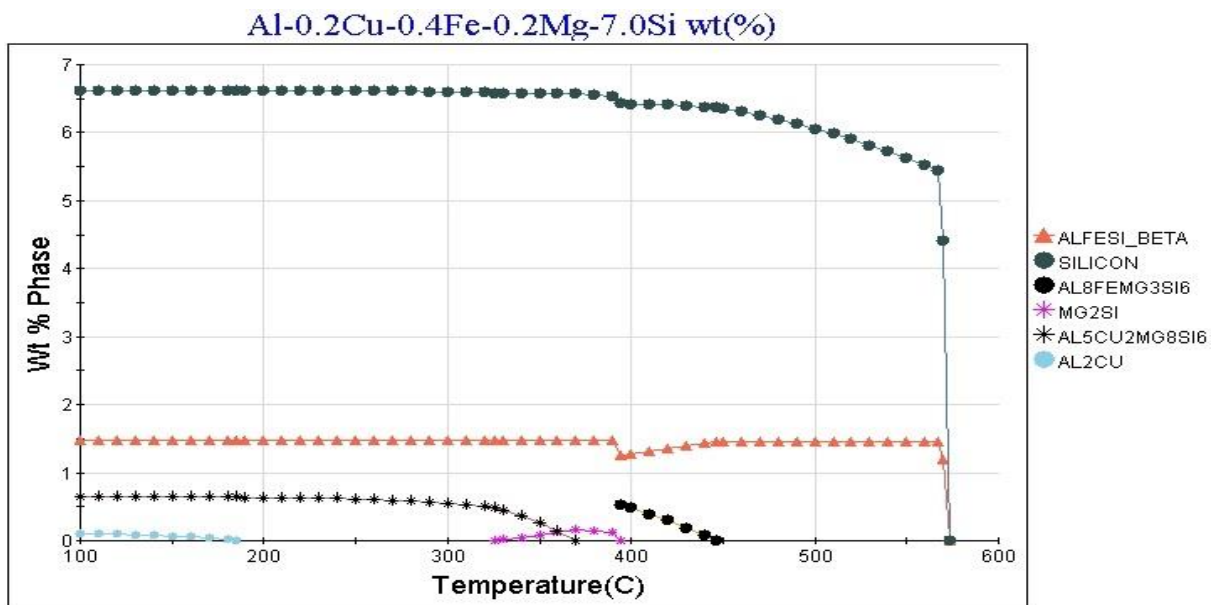


Fig. 5 Changes in intermetallic phases

**C. Effect of mold materials and pouring temperature on % Porosity and Hardness.**

The % porosity and hardness of the specimens produced at different pouring temperatures were measured and the results are shown in Fig. 6 and Fig. 7.

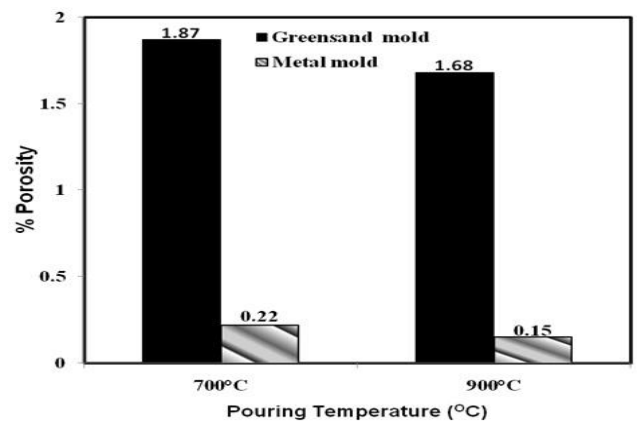
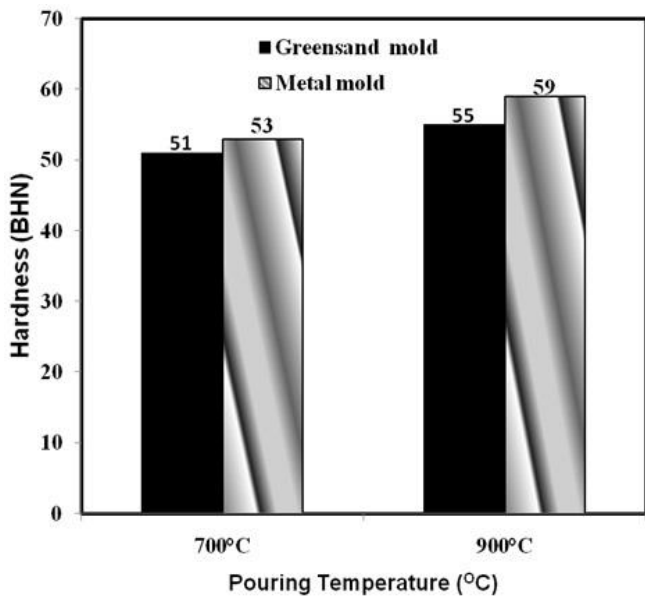
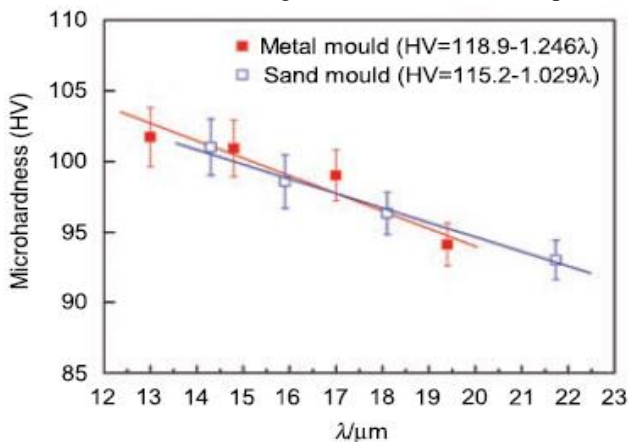


Fig. 6 % Porosity of LM25 alloy at different pouring temperatures



**Fig. 7 Brinell hardness of LM25 alloy samples at different pouring temperatures and cooled in the metal mold and sand mold, respectively**

The type of mold material is a major factor in reducing %porosity. From Fig. 6 it is clearly evident that the % porosity decreases with increasing pouring temperature and is lowest for metal mold casting. The SDAS also influences the size of eutectic Si and porosity. Finer SDAS leads to sound casting by reducing the porosity and the size of eutectic Si, which solidifies in between dendrite arms [17]–[21]. The hardness of the specimens produced at different pouring temperatures was measured and the results are shown in Fig. 7. It can be seen that the hardness increases with increasing pouring temperature. Moreover, the hardness of the metal mold casting alloy is higher than that of sand mold casting alloy at the same pouring temperature. A high pouring temperature generally increases the nucleating spots in the superheated melt and refines the microstructure [16]. The refined microstructures can be seen in Fig. 3(a) and 3(b). The refined microstructures improve the hardness of the alloy, implying that SDAS of as-cast alloys have an effect on hardness. From Fig. 8 it can be clearly seen that hardness decreases with increasing SDAS. The relationship between

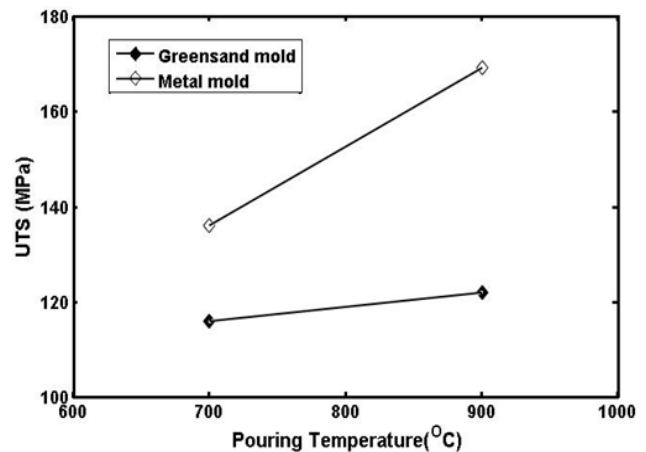


hardness and SDAS at air cooling and sand cooling is shown in Fig. These results are also similar to those obtained by Jing [22].

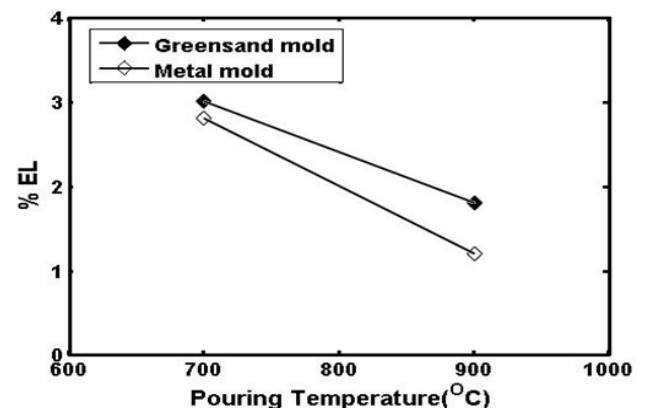
**Fig. 8 Relationship between hardness and SDAS (λ) [16].**

**D. Effect of mold materials and pouring temperature on tensile behaviour**

Fig. 9 shows the relationship between the tensile properties and the pouring temperature. It can be seen obviously from Fig. 9(a) that the ultimate tensile strength (UTS) increases with increasing pouring temperature, and the UTS of the metal mold casting specimens is higher than that of sand mold casting specimens because of the finer microstructure in metal mold casting specimens. The variation of the elongation (EL) with pouring temperature is given in Fig. 9(b). It is indicated that the elongation decreases with increasing pouring temperatures, and the elongation of the metal mold casting specimens is lower than that of sand mold casting because of the higher hardness. Various cooling rates during solidification lead to various microstructural characteristics of as-cast structures, which in turn can lead to different mechanical properties. Castings having a finer microstructure show better tensile and elongation properties, particularly for cast aluminum alloys, this improvement is related to a lower SDAS value. Studies on the effect of SDAS on tensile properties reported that the tensile strength and ductility decreases with increasing value of SDAS. The SDAS influences the size of eutectic Si and also affects the Ultimate Tensile Strength (UTS) and elongation.



(a)



(b)

**Fig. 9 Relationship between (a) UTS and (b) % EL with pouring temperature**



#### IV. CONCLUSIONS

The effect of foundry variables such as mold materials and pouring temperature on the microstructure, secondary dendrite arm spacing (SDAS) and mechanical properties of as-cast LM25 Al alloy have been determined. Metal mold castings have refined microstructure than sand mold castings owing to increased cooling rate/solidification rate. Hence, LM25 Al alloy has fine dendrite structure when casted in metal mold and also has better mechanical properties. Using thermodynamic modeling, the presence of intermetallic  $\text{CuAl}_2$  and Al-Cu-Mg-Si phases were confirmed. These intermetallic phases are responsible for better mechanical properties of the LM25 alloy. Metal mold castings also have less % porosity which leads to sound castings. The relationships between mechanical properties and SDAS with pouring temperature are presented in Fig. 10. It is clearly evident from Fig. 10 that pouring temperature has a marked effect on SDAS and mechanical properties. Higher pouring temperature leads to finer secondary dendrite arm spacing and as a result the UTS and Hardness of the alloy increases with a decrease in % elongation.

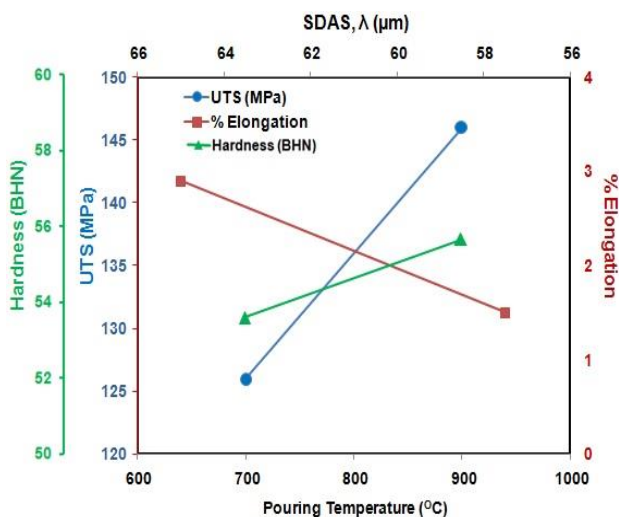


**Fig. 10 Relationship between mechanical properties and SDAS with pouring temperature**

#### REFERENCES

- [1] P.K.Mallick, fiber reinforced composites Materials, Manufacturing and design, CRC Press Taylor and Francis Group P.No:70(2010).
- [2] EEA Report: Aluminum Usage in Cars, 2008.
- [3] V. Suresh, R. Maguteeswaran, R. Sivasubramaniam, D. Shanmuga Vadivel, "Micro Tensile Behaviour of LM25 Aluminium Alloys by Stir Cast Method Compared with Finite Element Method", International Journal of Research in Mechanical Engineering, Volume 1, Issue 1, July-September, 2013, pp.111-116, www.iaster.com, ISSN Online:2347-5188 Print: 2347-8772
- [4] <http://www.azom.com/article.aspx?ArticleID=75>
- [5] Z. Li, A.M. Samuel, F.H. Samuel, C. Ravindran, S. Valtierra H.W. Doty, Mater. Sci. Eng., A 367 (2004) 96-110.
- [6] Z. Li, A.M. Samuel, F.H. Samuel, C. Ravindran, H.W. Doty, S. Valtierra, Mater. Sci. Eng., A 367 (2004) 111-122.
- [7] M. Zeren, J. Mater. Process. Technol. 169 (2005) 292-298. R. Torres, J. Esparza, E. Velasco, S.Garcia-Luna, R. Colas, Int. J. Microstructure and Materials Properties, 1 (2006) 129-138.
- [8] J. E. Gruzleski, B. M. Closset, The treatment of liquid aluminium-silicon alloys, 3rd ed., American Foundryman's Society, Inc. Des Plaines, Illinois, 1990.
- [9] L. Ananthanarayanan, J. E. Gruzleski, AFS Transactions, 141(1992) 383-391.
- [10] H. G. Kang, H. Miyahara, B. Ogi in: Proceeding of the 3rd Asian Foundry Congress '95 Eds.

- [11] Lee Z.H., Hong C.P., Kim M.H., The Korean Foundrymen's Society 1995, p. 108.
- [12] K. Rhadhakrishna, S. Seshan, M. R. Seshadri, AFS Transactions 88 (1980) 695-702.
- [13] J. Pavlović-Krstić, R. Bähr, G. Krstić, S. Putić, "The effect of mold temperature and cooling conditions on the size of secondary dendrite arm spacing in Al-7Si-3Cu alloy", MJOM Vol 15 (2) 2009 p. 105-113.
- [14] S. Hasse, editor of Gießerei-Lexikon, Schiele und Schön, publishing house for technical literature, Berlin
- [15] ASTM Standard B557, 1984, "Standard Test Methods for Tension Testing Wrought and Cast Aluminum- and Magnesium-Alloy Products," ASTM International, West Conshohocken, PA, 2003, DOI: 10.1520/B0557-10, www.astm.org.
- [16] Xiaowu HU, Fanrong AI and Hong YAN, "Influences of pouring temperature and cooling rate on microstructure and mechanical properties of casting Al-Si-Cu aluminum alloy", Acta Metall. Sin.(Engl. Lett.)Vol.25 No.4 pp272-278 August 2012
- [17] M. C. Flemings, Solidification Processing, McGraw-Hill, Inc, USA, 1974.
- [18] W. Kurz, D.J. Fisher, Fundamentals of solidification, Trans.Tech. Publications, Switzerland-Germany-UK-USA, 1984.
- [19] K. Rhadhakrishna, S. Seshan, M. R. Seshadri, AFS Transactions 88 (1980) 695-702.
- [20] B. Zang, M. Garro, C. Tagliano, Mater. Sci. Technol., 21 (2003) 3-8
- [21] C. H. Caceres, C. J. Davidson, J.R. Griffiths, Mater. Sci. Eng., A 197 (1995) 171-179.
- [22] T. Jing, Simulations during the Process of Solidification (Publishing House of Electronics Industry, Beijing, 2002)